

Multiple X-ray reflection from ionized slabs

R. R. Ross^{1*}, A. C. Fabian² and D. R. Ballantyne²

¹*Physics Department, College of the Holy Cross, Worcester, MA 01610, USA*

²*Institute of Astronomy, Madingley Road, Cambridge CB3 0HA*

4 November 2018

ABSTRACT

Multiple reflection of X-rays may be important when an accretion disc and its hot corona have a complicated geometry, or if returning radiation due to gravitational light bending is important, or in emission from a funnel such as proposed in some gamma-ray burst models. We simulate the effects of multiple reflection by modifying the boundary condition for an X-ray illuminated slab. Multiple reflection makes the soft X-ray spectrum steeper (softer) and strengthens broad emission and absorption features, especially the K-shell features of iron. This may be important in explaining the spectra of sources such as the Narrow-Line Seyfert 1 galaxy 1H 0707–495.

Key words: line: formation – galaxies: active – X-rays: galaxies – X-rays: general – galaxies: individual: 1H 0707–495

1 INTRODUCTION

The hard X-ray emission from luminous Seyfert 1 galaxies is often modelled as due to an optically-thin corona above a dense accretion disc. This model successfully accounts for the reflection component often found in the spectra of these objects (Pounds et al. 1990). The dense optically-thick accretion disc is often assumed to be relatively cold, with iron only weakly ionized (e.g. George & Fabian 1991; Matt, Perola & Piro 1991; Magdziarz & Zdziarski 1995). Sometimes however it may be highly ionized by the irradiating X-rays, resulting in a more complex spectrum (Ross & Fabian 1993; Życki et al. 1994; Ross, Fabian & Young 1999; Nayakshin, Kazanas & Kallman 2000; Ballantyne, Ross & Fabian 2001; Róžańska et al. 2002). Generally the disc is assumed to be flat.

Recent numerical simulations of luminous accretion discs (Turner, Stone & Sano 2002), particularly when radiation pressure is important, suggest that they are clumpy, irregular and possibly corrugated. In this case, if the corona lies close to the disc, the solid angle subtended by the disc at the corona may be much higher than 2π , the value for a flat disc, and the reflection spectrum itself may be reflected. This will certainly happen if the disc is corrugated and the corona lies close to the bottom of corrugations. The observer may then not see any direct emission from the corona but only multiply-scattered flux. (Rapid variability of an AGN requires that any such corrugations be on a relatively small spatial scale.)

We attempt here to simulate multiply-scattered reflection spectra for ionized discs in a simple generic manner using the code described by Ross & Fabian (1993). Multiply-scattered reflection spectra have been invoked as one explanation (Fabian et al. 2002) for the remarkable spectrum of the Narrow Line Seyfert 1 galaxy

1H 0707–495 observed by XMM-Newton (Boller et al. 2002). They might also be relevant if the accretion disc extends well within 6 Schwarzschild radii so that returning radiation due to light bending by the strong gravity of the black hole is important (Cunningham 1975; Martocchia, Matt & Karas 2002). Multiple reflection is expected naturally if the accretion flow consists of clouds rather than a disc (e.g. Celotti, Fabian & Rees 1992; Collin-Souffrin et al. 1996; Malzac 2001). Multiple reflection could also be important in hypernova models for Gamma-ray bursts (Mészáros 2001), in which the emission is surrounded by ejecta.

We expect that multiple reflection will enhance both broad absorption and emission features in the spectrum, relative to single reflection spectra. The net effect is to produce a considerably steeper (softer) spectrum with pronounced broad spectral features around the K-shell emission of iron and other elements.

2 THE MODEL AND METHOD

As an idealized model, let us consider that the hard continuum originates from close to the bottom of a well or hole. If the opening at the top subtends an effective solid angle Ω as seen from the bottom, then a fraction $\varepsilon = \Omega/2\pi$ of the emitted radiation escapes directly; the rest is scattered, absorbed and reflected by the material in the sides and bottom of the well. To a crude approximation, this reflected flux has a similar probability of escaping, with the rest striking the surfaces within the well. We model the multiple reflection process by simply introducing a partially reflecting mirror above a flat slab. A detailed model would involve knowledge of the precise geometry envisaged, but we expect that our simple model will give us a good qualitative guide to what the observer would expect to detect. If ε is small, an observer may see only the

* rross@holycross.edu

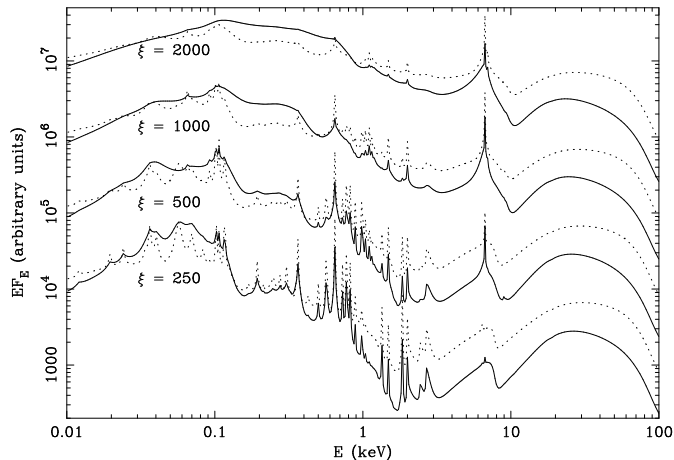


Figure 1. Observed spectra resulting from multiple reflection with escape fraction $\varepsilon = 0.25$ (solid lines) and from a single reflection (dotted lines) for four different values of the ionization parameter ξ . Spectra for different values of ξ have been offset vertically for clarity.

multiply-reflected flux, and it is this reprocessed radiation only that we discuss.

In detail, we treat a surface layer of gas with hydrogen number density $n_{\text{H}} = 10^{15} \text{ cm}^{-3}$ and Thomson depth $\tau_{\text{T}} = 10$. The outer surface is illuminated by “direct” radiation in the form of a power law with photon index $\Gamma = 2$ and with total flux F_0 (from 1 eV to 100 keV) corresponding to a specified ionization parameter

$$\xi = \frac{4\pi F_0}{n_{\text{H}}}. \quad (1)$$

The penetration of the illuminating radiation and the Compton-thick transfer of the diffuse radiation produced via scattering or emission within the gas are treated as described by Ross & Fabian (1993). At each step in the radiative transfer calculation, the diffuse radiation emerging from the outer surface is calculated as described by Foster, Fabian & Ross (1986). Only a fraction ε of this emergent flux, however, is allowed to escape to distant regions. The remaining fraction $(1 - \varepsilon)$ of the emergent flux is assumed to be reflected back onto the surface, so it is added to the “direct” radiation that illuminates the surface. The transfer calculation proceeds until the radiation field relaxes to a steady state, at which point the portion of the total emergent flux that actually escapes equals the total “direct” illumination.

3 RESULTS

We have calculated multiple-reflection models with direct illumination corresponding to $\xi = 250, 500, 1000$ and 2000 . For each value of the ionization parameter, models were produced with the emergent radiation having escape fractions of $\varepsilon = 0.25, 0.50, 0.75$ and 1.00 . Here $\varepsilon = 1$ corresponds to escape of all emerging radiation with no reflection back onto the surface, and these results are similar to those of Ross, Fabian & Young (1999).

Figure 1 shows the observed spectrum when only 25% of the emergent radiation actually escapes (and 75% is reflected back) in comparison with the spectrum without multiple reflection. Multiple reflection reduces the escaping flux for $E > 1 \text{ keV}$ by increasing the probability that such photons will be absorbed before ultimately escaping. In addition, it changes the *shape* of the observed spectrum. To make this clearer, Figure 2 shows the same two spec-

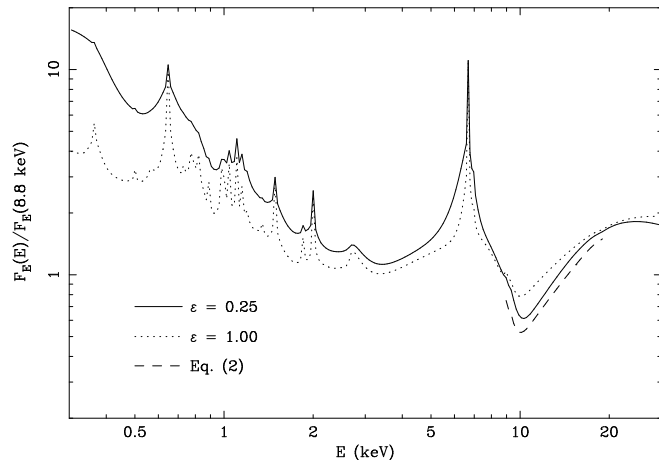


Figure 2. Spectra for $\xi = 1000$ renormalized by dividing the escaping flux $F_E(E)$ by the corresponding value at $E = 8.8 \text{ keV}$. The solid line is the result for multiple reflection with $\varepsilon = 0.25$, while the dotted line is the result for a single reflection ($\varepsilon = 1$). The dashed line shows the approximate shape of the Fe K-absorption feature for $\varepsilon = 0.25$ predicted using Eq. (2).

tra for $\xi = 1000$, but with each spectrum renormalized relative to the corresponding escaping flux at 8.8 keV (just below the K-edge of Fe XXV). The multiple-reflection spectrum exhibits a relatively deeper Fe K-edge, a stronger and broader Comptonized Fe K α line, and a steeper spectrum in soft X-rays ($\sim 1 \text{ keV}$).

An approximate test can be made of the accuracy of our method. Consider a photon energy for which the illuminated material is essentially a pure absorber and coherent scatterer—that is, there is no emission due to absorbed or scattered radiation at other photon energies. Let A be the albedo for a single reflection by the material. Then, if the probability of escape after each reflection is ε , the net albedo produced by multiple reflection is

$$\begin{aligned} A_{\text{net}} &= \varepsilon A + \varepsilon(1 - \varepsilon)A^2 + \varepsilon(1 - \varepsilon)^2 A^3 + \dots \\ &= \frac{\varepsilon A}{1 - (1 - \varepsilon)A} \end{aligned} \quad (2)$$

Fig. 2 shows the results of applying this formula to energies around the K-edge of iron, where it is approximately valid, for $\varepsilon = 0.25$. Eq. (2) predicts a slightly deeper absorption feature than our multiple-reflection calculation because it does not take into account incoherent Compton scattering of higher-energy photons, which partially fills in the absorption feature (see Ross, Weaver & McCray 1978).

Figures 3 and 4 provide another way of visualizing the changes that multiple reflection produce in the observed spectrum. In each case, the ratio of the flux escaping after multiple reflections to the flux escaping after a single reflection is shown as a function of photon energy. On average, decreasing the escape fraction ε decreases the entire spectrum above $\sim 1 \text{ keV}$. As ε decreases, however, the broad Fe K-absorption feature decreases by a larger amount than the X-ray spectrum as a whole, so that the *relative* strength of this feature is enhanced. On the other hand, as ε decreases, the broad, Comptonized Fe K α emission feature is suppressed less than the X-ray spectrum as a whole, so that this emission feature is also enhanced. At high ionization parameters ($\xi = 2000$ and 1000 ; Fig. 4), multiple reflection suppresses the narrow central core of the Fe K α line, since there is a deep, highly-ionized surface layer that Compton scatters line photons that reenter it. At the lowest ionization parameter ($\xi = 250$; Fig. 3), a decrease in ε enhances the Fe XXV line core at 6.7 keV and suppresses

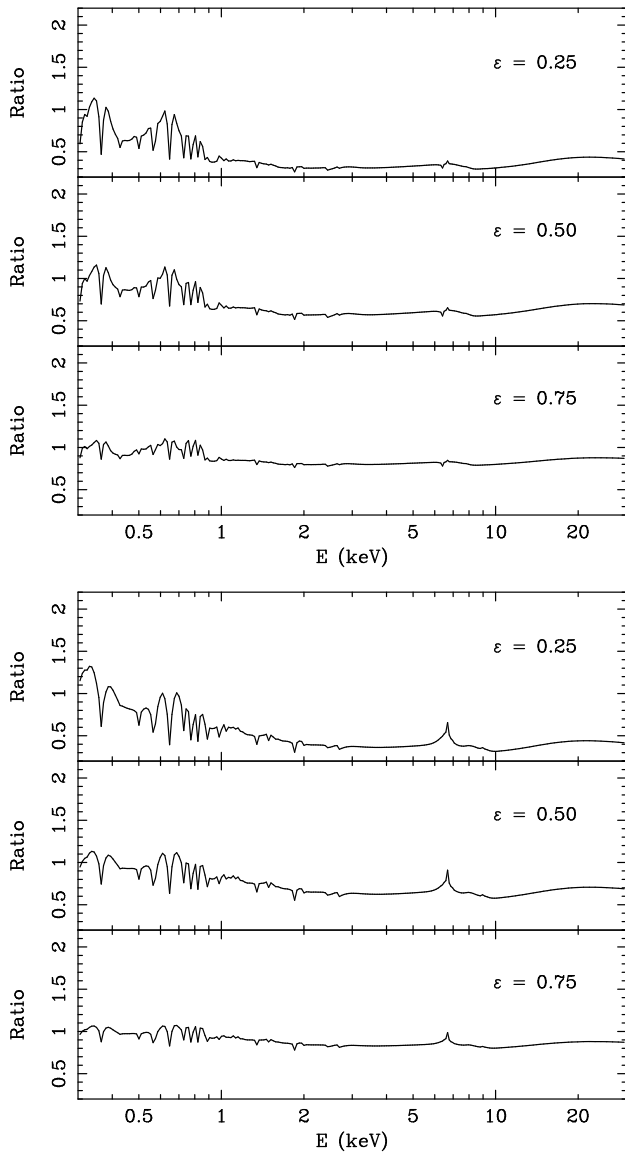


Figure 3. Ratio of the observed flux after multiple reflection with escape fraction ε to the observed flux after a single reflection. The upper panel shows the results for $\xi = 250$; the lower panel shows the results for $\xi = 500$.

the “neutral” iron line at 6.4 keV, since multiple reflection increases the effective ionization potential by increasing the total flux incident on the surface. In the soft X-ray region, the overall slope of the ratio presented in Fig. 3 or 4 steepens as ε decreases, indicating that multiple reflection steepens the observed spectrum compared to that resulting from a single reflection.

4 DISCUSSION

Multiple X-ray reflection creates a steep soft X-ray spectrum and a strong, broad, iron absorption/emission feature. The power lost from the harder energies above ~ 1 keV emerges at lower energies, principally in the 0.05–1 keV band. Overall the spectra resemble those from slightly higher ionization parameters and much higher abundances (Ballantyne, Fabian & Ross 2002).

A relativistically blurred version of the spectrum for $\varepsilon = 0.25$

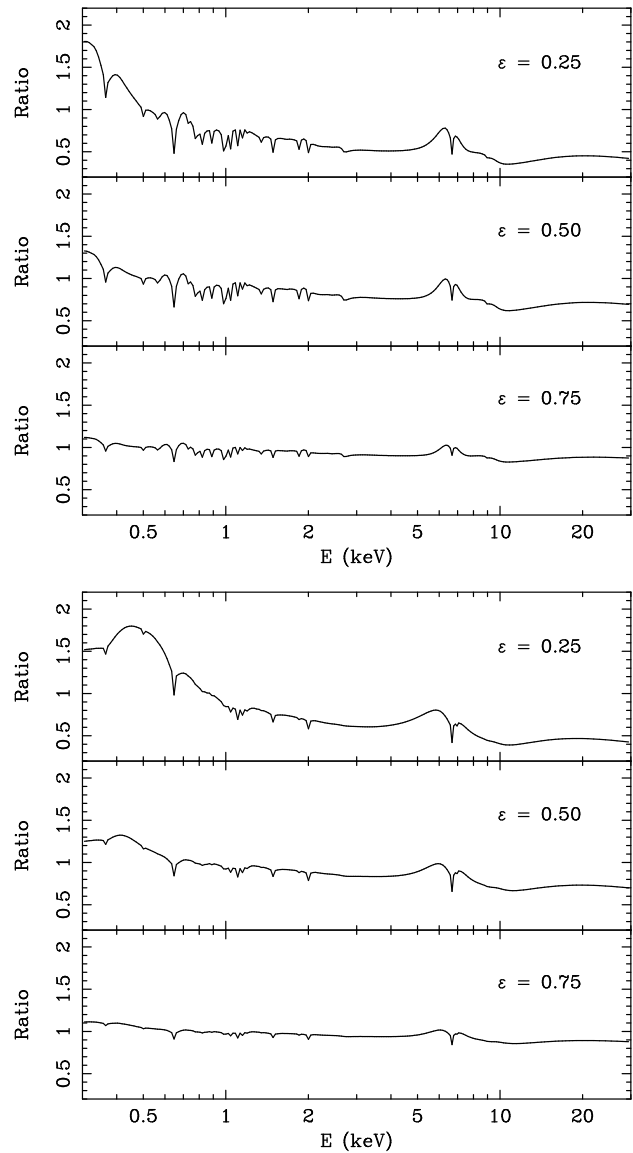


Figure 4. Flux ratios as in Fig. 3, except for $\xi = 1000$ (upper panel) and for $\xi = 2000$ (lower panel).

and $\xi = 2000$ is shown in Figure 5. That has been used to simulate what would be observed with the XMM-Newton EPIC pn CCD, and this is also displayed in Fig. 5 in the form of a ratio to an incident power-law of photon index 2.7. The result compares well to the spectrum of 1H 0707–495 found by Boller et al. (2002). If we fit the simulated spectrum from 2–10 keV with a power-law plus a broad gaussian line, then we find that the best-fitting line has a central energy of 4.8 keV, a width of 1.5 keV and an equivalent width of about 6 keV. Positive residuals remain over the 6–7 keV band. It is not our intention to carry out a detailed fit to the data of 1H 0707–495, which would require a comprehensive grid of models, but merely to confirm that multiple reflection may be relevant there, as suggested by Fabian et al. (2002). Since the spectrum of 1H 0707–495 is unusual, multiple reflection may occur only occasionally among Narrow Line Seyfert 1 galaxies, and/or the primary continuum may be seen in addition to the reprocessed component most of the time.

Multiple reflection can be important when light bending is strong enough to cause part of the reflected spectrum to return to

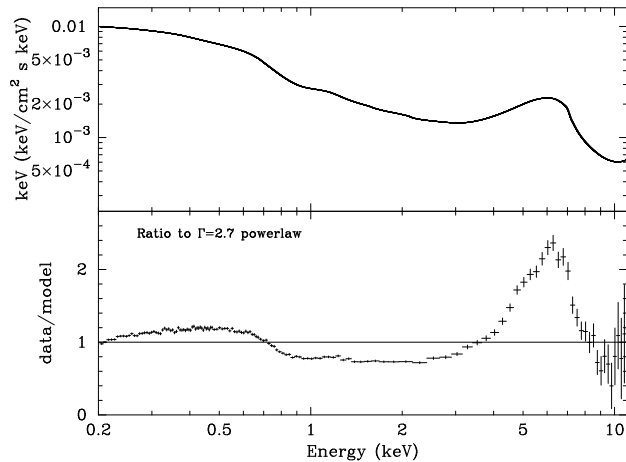


Figure 5. Top: Model spectrum for $\varepsilon = 0.25$ & $\xi = 2000$ relativistically blurred by a kernel appropriate (Laor 1991) for a disk inclined at 30 deg to the line of sight and extending from 3 to 100 gravitational radii ($3\text{--}100 \times GM/c^2$). Bottom: Ratio of fake data obtained by simulating the above model for the EPIC pn CCD for 40 ks (and intensity appropriate for 1H 0707–495) to a power-law model of photon index 2.7.

the disk. This occurs close to the centre of disks around maximally spinning Kerr black holes (Martocchia & Matt 1996; Dabrowski et al 1997; Dabrowski & Lasenby 2001; Martocchia, Matt & Karas 2002). Strong X-ray reflection has also been invoked (Vietri et al 2001; Ballantyne & Ramirez-Ruiz 2001) for the production of X-ray lines seen in some gamma-ray bursts (e.g. Piro et al 2000). If the emission is from a funnel geometry (Rees & Meszaros 2000; McLaughlin et al 2002) then the calculations presented here could be relevant. Lower abundances are implied than obtained from single reflection calculations.

5 ACKNOWLEDGEMENTS

The authors thank the anonymous referee for helpful comments. ACF thanks the Royal Society for support, RRR acknowledges support from the College of the Holy Cross, and DRB acknowledges financial support from the Commonwealth Scholarship and Fellowship Plan and the Natural Sciences and Engineering Council of Canada

REFERENCES

- Ballantyne D.R., Ross R.R., Fabian A.C., 2001, MNRAS, 327, 10
 Ballantyne D.R., Fabian A.C., Ross R.R., 2002, MNRAS, 329, L67
 Ballantyne D.R., Ramirez-Ruiz E., 2001, ApJ, 559, L83
 Boller Th. et al. 2002, MNRAS, 329, L1
 Celotti A., Fabian A.C., Rees M.J., 1992, MNRAS, 255, 419
 Collin-Souffrin S., Czerny B., Dumont A.-M., Życki P.T., 1996, A&A, 314, 393
 Cunningham C.T., 1975, ApJ, 202, 788
 Dabrowski Y., Fabian A.C., Iwasawa K., Lasenby A.N., Reynolds C.S., 1997, MNRAS, 288, L11
 Dabrowski Y., Lasenby A.N., 2001, MNRAS, 321, 605
 Fabian A.C., Ballantyne D.R., Merloni A., Vaughan S., Iwasawa K., Boller Th., 2002, MNRAS Letters, in press (astro-ph/0202297)

- Foster A.J., Fabian A.C., Ross R.R., 1986, MNRAS, 221, 409
 George I.M., Fabian A.C., 1991, MNRAS, 249, 352
 Laor A., 1991, ApJ, 376, 90
 Magdziarz P., Zdziarski A.A., 1995, MNRAS, 273, 837
 Malzac J., 2001, MNRAS, 325, 1625
 Martocchia A., Matt G., 1996, MNRAS, 282, L53
 Martocchia A., Matt G., Karas V., 2002, A&A, 383, L23
 McLaughlin G.C., Wijer R.A.M., Brown G.E., Bethe H.A., 2002, MNRAS, 567, 454
 Matt G., Perola G.C., Piro L., 1991, A&A, 247, 25
 Mészáros P., 2001, Science, 291, 79 (astro-ph/0102255)
 Nayakshin S., Kazanas D., Kallman T.R., 2000, ApJ, 537, 833
 Piro L. et al 2000, Science, 290, 955
 Pounds K.A., Nandra K., Stewart G.C., George I.M., Fabian A.C., 1990, Nature, 344, 132
 Rees M.J., Mészáros P., 2000, ApJ, 545, L73
 Rees M.J., Netzer H., Ferland G.J., 1989, ApJ, 347, 640
 Ross R.R., Fabian A.C., 1993, MNRAS, 261, 74
 Ross R.R., Fabian A.C., Young A.J., 1999, MNRAS, 306, 461
 Ross R.R., Weaver R., McCray R., 1978, ApJ, 219, 292
 Różańska A., Dumont A.-M., Czerny B., Collin, S., 2002, MNRAS, 332, 799
 Turner N.J., Stone J.M., Sano T., 2002, ApJ, 566, 148
 Vietri M., Ghisellini G., Lazzati D., Fiore F., Stella L., 2001, ApJ, 550, L43
 Życki P.T., Krolik J.H., Zdziarski A.A., Kallman T.R., 1994, ApJ, 437, 597

This paper has been typeset from a \TeX \LaTeX file prepared by the author.